Soft Matter

Accepted Manuscript

ROYAL SOCIETY OF CHEMISTRY

www.rsc.org/softmatter

Journal Name

RSCPublishing

ARTICLE

Tuning self-assembly in elastin-derived peptides

Cite this: DOI: 10.1039/xoxxoooooox

Brigida Bochicchio,[*a] Antonietta Pepe,[a] Maria Crudele,[a] Nicola Belloy,[b] Stephanie Baud[b] and Manuel Dauchez[b],

Received ooth January 2012,
Accepted ooth January 2012

DOI: 10.1039/xoxxoooooox

www.rsc.org/

Elastin-derived peptides are gaining increasing interest as potential biomaterials. Previous studies have demonstrated that short elastin-derived peptides are able to self-assemble into fibrils as the entire elastin protein. The motif responsible for that is the XGGZG motif at least three-fold repeated. In this work we have synthesized and studied, at molecular and supramolecular level, four pentadecapeptides obtained by switching the X and Z residue with leucine and/or valine. We found that the four peptides formed different supramolecular structures corresponding to specific molecular conformations. Our results show that not only the residue type but also the exact position occupied by the residue in the motif is crucial in driving the self-aggregation. The aim of this work is to put the basis for designing elastin–derived peptides with tunable supramolecular architecture.

INTRODUCTION

The research on bioinspired materials is an emerging and interdisciplinary field focusing on developing a fundamental understanding of the synthesis, directed self-assembly and hierarchical organization of natural occurring materials for bioengineering new artificial materials for diverse applications ranging from regenerative medicine to electronics.[1] Materials and devices from carbohydrates, RNA/DNA and proteins gained great interest in the field of biomaterials as these biopolymers represent the building blocks of life.[2] They are appealing for medical use owing to their biocompatibility. Concerning the protein-based materials, one of the more interesting characteristics endowing recently developed biomaterials is the ability to self–aggregate. The DNA-recombinant techniques together with the Solid Phase Peptide Synthesis (SPPS) technology prompted the development of high molecular weight polypeptides and of shorter peptides, respectively.[3-4] As a matter of fact, although long polypeptides play a prominent role for their outstanding mechanical properties, even short aromatic di- and tri-peptides are interesting potential biomaterials for their impressive self-assembling properties.[5-7] Natural proteins have inspired the design of peptides having sequences considered significant for the biological function of the protein. The main function of elastomeric proteins is to confer rubber-like elasticity to organs and tissues thus enabling them to undergo high deformation without rupture and to return to their original state on removal of the stress.[8] Elastin is an insoluble extracellular matrix protein that in the form of fibres is responsible for elasticity of organs and tissues such as lungs and skin also in humans. The presence of repetitive sequences favoured a synthetic approach toward the elucidation of the molecular structure of elastin[8]. Experimental and theoretical studies evidenced the crucial importance of glycine residues for the mechanism of elasticity not only of elastin but also of several elastomeric proteins.[9,11]Tamburro and co-workers focused their attention on the GXGGZ motif (X, Z = V, L) which is n-fold repeated in elastin of different species and able to form elastin-like supramolecular structures constituted of twisted-rope fibrils.[12] The first attempt to obtain longer polypeptides was made by polycondensation reaction on the XGGZG monomer. The permutation XGGZG instead of GXGGZ was done in order to avoid racemization during the polycondensation step.[13] Further studies on poly(XGGZG) sequences suggested the influence of X and Z residue[14-15] and of the solvent on self-assembly.[16] However, the main pitfall of these peptides was constituted by the polydisperse molecular weight responsible for the presence of a batch of peptides having different degree of polymerization varying from three to five blocks[17]. In order to overcome this limit, Kumashiro and co-workers studied $(LGGVG)_6$ by solid-state NMR.[18] However, the first deep investigation on a

monodisperse molecular weight polypeptide containing the XGGZG motif has been only recently achieved.[19] Inspired by these results showing also the peptide cytocompatibility, we have synthesized by solid phase peptide synthesis, four polypeptides having the XGGZG motif three-fold repeated with the X and Z residues constituted of Valine and/or Leucine.Both of these residues are among the most abundant residues in elastin, occupying in this pattern the first and/or fourth position (Table I). The final aim of the work is to gain useful insights in the relationship between the primary structure and the self–aggregation properties because the understanding of the self-aggregation process is mandatory for the design of bioinspired materials having predictable architectures. The detailed study of the secondary structure of each peptide is presented through CD, NMR, and MD data in the experimental conditions shown in Table II. The aggregates were formed in TBS buffer and studied by AFM and FTIR as well. We conclude that, among the synthesized peptides, $(VGGVG)_3$ and $(LGGVG)_3$ are the most able to self-aggregate into regularly wrapped nanostructured fibres.

Results and Discussion

Self-aggregation

Ultraviolet Spectroscopy and Atomic Force Microscopy

Turbidity assays have been used to develop some basic understanding of aggregation kinetics even if suffering from the tendency of the largest aggregates to dominate the signal[20,21]. However, the time course of turbidity furnishes important qualitative information on the ability of a specific peptide to self-aggregate. The turbidity of the sample is recorded as a function of time at a given wavelength where the solution components do not absorb light. As a matter of fact, the term Turbidity on Apparent Absorbance (TAA) is more suitable than Absorbance in a turbidity graph. Herein, the TAA of each peptide is measured by turbidity technique. TBS buffer solution was used in order to speed up the kinetic measurements. As a matter of fact, $(VGGVG)_3$ in water gave rise to a sigmoidal curve after one week (data not shown) *vs* one day shown in buffer (Fig. 1). The end of the turbidimetric assay is defined by the measurement of a constant TAA value (plateau in Fig. 1). We will not discuss the absolute value of the apparent absorbance of the peptide, as it is more related to the aggregate dimensions than to the specific propensity of the peptide to self-aggregate while the physical transformation of a limpid solution in a cloudy suspension will be considered. As evidenced in Fig. 1 all peptides show a sigmoidal rise of the TAA ending in a plateau thus suggesting that all of them are able to self–aggregate. As a matter of fact, a turbid suspension was visible in the cuvette at the end of the measurements. At the end of the time course measurements, the aggregates were observed by atomic force microscopy (Fig. 2). Straight rods interacting side-by-side and 70 nm wide are visible for $(VGGLG)_3$ (Fig. 2a) and short fibrils organized in flocks were detected for $(LGGLG)_3$ (Fig. 2b). The AFM micrograph of $(VGGVG)_3$ from TBS solution shows tangled filaments forming a branched ensemble (Fig. 2c). Furthermore, the AFM micrographies of $(VGGVG)_3$ prepared in water and showing multiple layers of helically wound fibres were previously characterized[22] thus suggesting the high ordered supramolecular organization for this peptide A layer with regularly intertwined fibres is found for $(LGGVG)_3$ and shown in Fig. 2d. Fibres have different level of brightness modulation corresponding to different height modulation. Although heights differ, the long and thin fibres of $(LGGVG)_3$ appear homogeneous in their morphology and characterized by very regular helical pitches having a periodicity of about 100 nm (Inset of Fig. 2d).

Fourier Transformed Infrared Spectroscopy

In order to complete the study of aggregated peptides solid-state Fourier Transformed Infrared Spectroscopy (FTIR) was carried out. The peptides were analyzed both in lyophilized powder, giving insights into the pre-fibrillar state and in aggregated form. Decomposed Amide I and II regions are shown for all peptides in Fig. 3. At a first look, FTIR spectra of the lyophilized form (Figures 3a, c, e, g) are very different from those in the aggregated form (Figures 3b, d, f, h). As a matter of fact, it is evident for all peptides in the aggregated state that FTIR Amide I curve is strongly asymmetric. This is due to the dominance of a low wavenumber component at 1629–1630 cm^{-1} usually assigned to cross-β structures.[23] FTIR decomposed spectrum of lyophilized $(VGGLG)_3$ shows a dominant component at 1655 cm^{-1} indicative of unordered conformation (Fig. 3a).[24] The remaining components are comparable and assigned to the water contribution, 1639 cm^{-1}, to PPII conformation, 1670 cm^{-1}, and to β-turns, 1685 cm^{-1}.[24-27] The Amide II region of the lyophilized peptide is characterized by the presence of three different components. The bands at 1521 and 1557 cm^{-1} are indicative of hydrogen bonded NH groups compatible with the presence of β-turns, while the other at 1541 cm^{-1} is tentatively assigned to unordered conformations The aggregated state shows a prominent component at 1630 cm^{-1} indicative of a strongly hydrogen bonded carbonyl group (Fig.3b) . The remaining components at 1638 and 1655 cm^{-1} could be assigned to water and random coil absorptions, respectively. Finally, the band at 1671 cm^{-1} is indicative of the presence of PPII conformation and the small component at 1690 cm^{-1} could be assigned to β-turns. The aggregated peptide shows for Amide II region a pattern similar to that described for the lyophilized peptide (Fig. 3a). Fig. 3c shows the FTIR of $(LGGLG)_3$ in the lyophilized state. The Amide I region shows only two components at 1654 and 1682 cm^{-1} assigned to unordered and β-turn conformation, respectively. The Amide II region shows two components at 1557 and 1528 cm^{-1} assigned to β-sheet conformations. The aggregated state of $(LGGLG)_3$ is shown in Fig. 3d. The component at 1629 cm^{-1} is indicative of strongly hydrogen bonded carbonyl groups compatible with the cross-β structure. Minor contributions from random coil and β-turns are discernible as suggested by the bands at 1655 and 1684 cm^{-1}, respectively. FTIR results of $(VGGVG)_3$ are shown

in Fig. 3h and infer the dominance of cross-β structures in the aggregated state, as elsewhere discussed.[14] The decomposed FTIR spectra of $(LGGVG)_3$ are shown in Figures 3g and 3h. The lyophilized sample (Fig. 3g) is characterized by three components of comparable intensities at 1639, 1664 and 1686 cm^{-1} indicative of the contributions of water, random coil and β-turn conformations, respectively. The Amide II decomposed band is populated by three components. The band at 1536 is indicative of the presence of β-sheet, the components at 1556 and 1517 cm^{-1} suggest the presence of antiparallel β-sheet conformation. The Amide I region of the aggregated state (Fig. 3h) is dominated by the band at 1630 cm^{-1} indicative of the cross-β structure. In the Amide II region an impressively strong and sharp component at 1552 cm^{-1} is visible together with a minor component at 1524 cm^{-1}, both of them assigned to β-sheet structures. Overall, at molecular level FTIR suggests for all peptides in the prefibrillar state the presence of different conformations such as PPII, β-turn and unordered conformations while in the aggregated state the presence of cross-β structure is ubiquitous in all peptides but is dominant in $(VGGVG)_3$ and $(LGGVG)_3$ (Table III).

Molecular Studies

The secondary structure of the peptides was investigated in solution on unseeded peptides by MD, CD and NMR (Table II). The aim is to have useful insights into the not aggregated state of the peptides.

Molecular Dynamic Simulations

Numerical simulations were performed for each $(XGGZG)_3$ sequence in order to gain insights into the dynamical behaviour at the atomic scale of the peptides. As described in Fig. S1 of ESI† the radius of gyration fluctuates between a minimum of 5.7 and a maximum of 13.5 Å for all the investigated sequences. The radius of gyration values are compatible with a "small elastic peptide" dynamic behaviour characterized by the ability of the peptide to be in equilibrium between fully extended (maximum value of gyration radius) and "folded" (minimum value) conformations during the trajectories, as previously described.[28-30]

"Turn" is defined as Cα(i)–Cα(i+3) distance lower than 7 Å. The simultaneous orientation of both the (i+1) and (i+2) residues identifies the turn type. Molecular Dynamic (MD) analysis shows that $(VGGVG)_3$ and $(LGGLG)_3$ have a higher propensity to adopt this kind of local structure than $(VGGLG)_3$ and $(LGGVG)_3$. This can be assigned to an inherent behaviour of the sequence due to the lack of charged termini as described in MD protocol that could lead to biased folded peptide if not capped. Moreover, the amount of polyproline II (PPII) measured along the trajectory is located in the range from 8.12 to 14.81%. The specific conformation content for each residue was extracted from the coordinate files by using dihedral canonical values with either a ±30°or ±40° deviation. It is interesting to note that $(LGGLG)_3$ exhibits a propensity to give short helices involving 4 residues located at the edge of type I β–turn. Indeed, α-helix is located around the φ=-60°, ψ=-45° region of the Ramachandran map while type I β-turn is assigned with φ=-60°, ψ=-30° for (i+1) and with φ=-90°;ψ=0° for (i+2) residue, respectively. For both $(VGGLG)_3$ and $(LGGVG)_3$ the presence of switched V/L for the X and Z amino-acids lead to strong local conformations of turns, far away from β-strand and/or helix structures. Solvation of peptides (data not shown) may be responsible for this finding. Moreover, the lack of dedicated force field for elastomeric peptides and capped end termini could be responsible for the lack of distinguished results for these two peptides unlike it was observed with experimental data. The most important observation is that $(VGGVG)_3$ can give rise to a β–hairpin structure constituted of two β-strands connected by a turn. The β-strands are associated along the sequence to form locally a small β-sheet structure moving along the backbone during the simulation (Fig. 4). For clarity, the cartoon representation is used (strand in yellow, turn in cyan, coil in white) and the first Cα is symbolized as a black sphere for Val, white sphere for Gly and transparency for secondary structure elements. The transient β–sheet regions observed during the MD let us to propose the term of sliding β-sheets as a new model for the dynamic structures. The ends of the 15-mer remain free to move and thus should be able to interact with close 15-mer in order to guide the self-assembling process. The dynamical behaviour of these local β-sheets is under control of the intermediate turn moving along the chain. Previous experimental and theoretical results carried out on some elastin–derived peptides showed also labile β–turns able to interconvert each other thus giving rise to dynamic beta-turns sliding along the chain.[31] MD studies carried out on VGGVG and $(VGGVG)_2$ did not reveal the presence of sliding β-sheets thus suggesting that the peptide length is also crucial for the observation of sliding β-sheets (data not shown). Actually, we observe that some β-strands are associated along the sequence to form locally a small β-sheet structure only for $(VGGVG)_3$ constituted of 15 residues.

Circular Dichroism Studies

The Circular Dichroism (CD) studies were firstly carried out in TBS buffer as a function of time for $(VGGVG)_3$ (Fig. S2 of ESI†). However, the absorption of the buffer medium at low wavelength values, makes these spectra not very informative of the secondary structure of the peptide. This region is crucial for assessing the conformation adopted by the peptide because herein are found the bands diagnostic of specific conformations such as ⟨-helices, β-sheets and β-turn. As a matter of fact, the spectra recorded in TBS solution and showing only one negative band at 220 nm, are not informative. Therefore, the study is carried out at different temperatures and in different solvents such as water and 2,2,2–trifluoroethanol (TFE) that is a structure-inducing solvent promoting folded conformations such as beta-turn and alpha-helices. Figure 5a shows CD spectra of $(VGGLG)_3$. In aqueous solution the spectrum at 273 K shows a strong negative band at 194 and a small positive band at 214 nm. At 298 and 343 K both bands are reduced in intensity suggesting the presence of the PPII.[32,33] The CD

spectrum in TFE at 273 K is characterized by a small negative band at 195 nm, a positive bands at 210 nm and a small negative band at 228 nm of comparable intensities. The increase of the temperature to 298 and 343 K induces the slight reduction of the bands. These spectral findings are indicative of the presence of unordered conformations with little amount of β-turns.[33] CD spectra of $(LGGLG)_3$, Fig. 5b, are characterized by analogous curves to those observed in Fig. 5a. In aqueous solution, all of them show a strong negative band centred at 195 and a small positive one at 215 nm. The increment of the temperature induces a slight reduction of both bands suggesting the destabilization of the PPII helix at higher temperatures. In TFE, the CD spectra are mostly invariant with the temperature and are characterized by a tendency to adopt positive ellipticity values at 190 nm and by two negative bands at 200 and 230 nm. These CD spectra suggest the presence of dominant unordered conformations together with little amounts of β-turns. Interestingly, CD spectra of $(VGGVG)_3$, reported in Fig. 5c, are very different from those previously discussed. In aqueous solution they are indicative of the presence of the β-sheet conformation.[19] In TFE, the CD spectrum at 273K is characterized by a strong positive band at 199 nm and by a weak negative band at 217 nm. Even if the band at 217 nm is diagnostic of the β-sheet conformation, the positive band is 4 nm red-shifted if compared to an antiparallel β-sheet conformation and is more compatible with the presence of β-turns. The increase of the temperature to 298K induces a slight modification of the spectrum observed at 273 K with a reduction of the positive band and the increase of the negative one. On the other hand, at higher temperature the positive band strongly decreases as the negative band as well. The observed spectral features are due to the increasing contribution of unordered conformations dominant at high temperatures. Fig. 5d shows CD spectra of $(LGGVG)_3$ in aqueous solution. The spectral features are similar to those observed in Fig. 5a and 5b thus suggesting for this peptide analogous conformations. In TFE, Fig. 5d, the CD spectrum at 273 K indicates a strong positive band at 198 nm and a small negative one at 225 nm. The spectrum is diagnostic of a type II β-turn. The decrease of the temperature to 298 K induces the reduction of the bands that disappear at 343 K indicating the destabilization of the β-turn. On summarizing, CD studies demonstrate that $(LGGLG)_3$ and $(VGGLG)_3$ adopt mainly extended (PPII) and unordered conformations while $(VGGVG)_3$ and $(LGGVG)_3$ more folded structures such as β-turns. Additionally, $(VGGVG)_3$ is characterized also by the presence of the β-sheet structure in aqueous solution. These findings are in good agreement with previous studies showing that the elastin sequences ALGGGALG, LGAGGAG and LGAGGAGVL containing the simple dipeptide LG, were found to be structured according to the PPII conformation in aqueous solvent. On a smaller scale the same structure is adopted by the dipeptide LG, as ascertained by X-ray diffraction studies. Furthermore, the protected tripeptide Boc-VGG-OH was found to adopt a β–turn with VG at the corners. It is known that many much longer sequences of elastin contain well-established β-turns with XG sequences at the corners (X=V, L, A).[34]

Nuclear Magnetic Resonance Spectroscopy

As observed by CD spectroscopy, the $(XGGZG)_3$ peptides present significant differences in the population of conformations adopted, especially in TFE. In order to better define the structures of the $(XGGZG)_3$ peptides, NMR spectra in TFE-d_3/H_2O (80/20, v/v) at 298 K were recorded. In order to make comparable CD and NMR data, the CD spectra of $(VGGVG)_3$ were carried out also in TFE-d_3/H_2O (80/20, v/v) (Fig. S3 of ESI†). The CD spectra are similar to those obtained in TFE alone thus suggesting the presence of analogous conformations (Fig. 5c). Several NMR parameters useful for structure determination were assessed giving insights into the different conformations adopted by the peptides. The ^1H chemical shift assignments were accomplished following standard procedures, with minor changes due to the repetition of the XGGZG motif (Table S1-S4 of ESI†).[35] The chemical shifts of the Hα proton resonances of all peptides adopt values assigned to unordered conformations.[36] The $^3J_{NH\text{-}H\alpha}$ coupling constants of leucine residues are in the range 6.6-7.8 Hz, typically assigned to unordered or PPII conformations, while the valine show values in the range 8.2-8.8 Hz, suggesting a more extended conformation for these residues. Additionally, the temperature coefficient (TC) analysis of the amide protons shows reduced TC values for some specific residues, indicative of a reduced exposition to the solvent usually ascribed to the intramolecular hydrogen bonding. Asa matter of fact, $(LGGLG)_3$, $(LGGVG)_3$ and $(VGGVG)_3$ peptides show TC values for some amide protons in the range of 4.4-4.8 $ppbK^{-1}$, attributed to very weak H-bonds or to an equilibrium between turn and other conformations lacking in H-bonds. In the presence of β-turns, the lowered TC value is due to the presence of hydrogen-bonds between the amide proton of the fourth residue and the carbonyl group of the first residue of the turn. According to the TC values, two type of turns are proposed (Fig. 6), one containing the XGGZ sequence, having GG at the corners, observed for $(VGGVG)_3$ and $(LGGVG)_3$, and the other having the GXGG sequence with XG at the corners observed for $(LGGLG)_3$. Even if, intense sequential NOEs $d_{NN(i,i+1)}$ values and typical medium range NOE $d_{\alpha N(i,i+2)}$ are considered additional evidences of turn structures, in our case it was not possible to identify the typical medium range NOE $d_{\alpha N(i,i+2)}$ for all suggested turn structures, because of severe overlap in the glycine Hα proton region. From previous results on similar sequences we could infer that the XGGZ sequence adopts a type II β-turn while the GXGG sequence adopt usually a type I β-turn.[31,34] In accordance with CD and NMR results we propose for $(VGGVG)_3$ and $(LGGVG)_3$ type II β-turns. On the other hand, $(LGGLG)_3$ adopts transient type I and type II β-turns while $(VGGLG)_3$ does not adopt detectable turn structures. Finally, $(VGGVG)_3$ has the highest tendency to take β-strand structures as evidenced by the high $^3J_{NH\text{-}H\alpha}$ coupling constant (8.5-8.7 Hz) observed for the valine residues. These results are in full agreement with CD and MD studies.

From molecular to supramolecular structure

On the basis of microscopy studies, the four peptides form aggregates of different morphology (Fig. 2).These findings confirm previous studies carried out on analogous polypeptides obtained by polycondensation reactions of (XGGZG) monomers.[15] A rationale for that could be given by the specific residue in the sequence that play a pivotal role in driving the self-assembly. As a matter of fact, peptides containing valine have a high tendency to form regular fibres, mainly promoted by β-sheet structures[37],whereas leucine rich peptides are often involved in vescicles[1]. Accordingly, $(VGGVG)_3$ is prone to form regular and long fibers, while $(LGGLG)_3$ forms more irregular polymorphic flock-like aggregates. More controversial issue is $(LGGVG)_3$ and $(VGGLG)_3$ having identical composition but different sequence. When leucine occupies the first position of the XGGZG motif the related pentadecapeptide formed intertwined fibres while when it is in fourth position only rigid rods are found (Fig. 2).These experimental findings are corroborated by data from methods that rely on individual amino acid aggregation propensities. As a matter of fact, ZYGGREGATOR program,[38] a sequence-based method of predicting aggregation propensities of proteins, suggests for all peptides the tendency to self-aggregate (values above the ZAgg=1 threshold) in good agreement with turbidity data (Fig. 7). $(VGGVG)_3$ shows the highest propensity to self-aggregate (Fig. 7C) while $(LGGLG)_3$ has the less (Fig. 7B). Slight differences are observed for $(VGGLG)_3$ and $(LGGVG)_3$ reported in Fig. 7A and 7D, respectively, even if the second shows higher propensity toward self-assembly. A possible explanation for the different aggregates observed at supramolecular level could be given by the relationship among peptide sequence, secondary structures and aggregates morphologies of the peptides (Table III). While at molecular level the β-sheet conformation is an essential but not sufficient condition in order to obtain strongly intertwined fibrils, our studies infer the fundamental role of β-turns in driving the self-assembly. Both conformations, the β-sheet and the β-turns, are compatible with cross-β conformation[39] found for $(VGGVG)_3$ and $(LGGVG)_3$ (Table III). On the contrary, the extended and flexible PPII conformation is predominant in $(LGGLG)_3$ and $(VGGLG)_3$ peptides less inclined to form fibrils. Accordingly, the TANGO predictor[40], a prediction method using a statistical mechanics approach to make secondary structure predictions, applied to our peptides shows that the preferred conformation is β-turn and that $(LGGVG)_3$ follows $(VGGVG)_3$ while $(LGGLG)_3$ is the less prone to make turns (data not shown). In general terms, β-turn conformation plays an important role also in the nucleation mechanism of some aggregating sequences such as poly-Q peptides and their amyloids exhibiting antiparallel β-sheet secondary structure. Two possible models, aimed to shed light on how polypeptide sequences might be placed into antiparallel β-sheet structures were proposed for peptides longer than 15 residues. Both models invoke the presence of β-turn conformation as structure able to connect two β-strands. However, the two strands forming an antiparallel β-sheet are lying adjacently in the same plane in the β-hairpin model[41] while are rotated by about 90 degrees around its axis, so that they interact via the side chains and not via the polypeptide backbones in the β-arch model.[42] The importance of the β-turn in the dynamics of elastin peptides turned out also from MD studies, showing for the first time elastin peptides that form sliding β-hairpins with labile β-sheets moving along peptide sequence. On that basis, the sliding β-sheet model is conceived.

Experimental Section

Peptide synthesis, disaggregation and purification

The peptides were synthesized by SPPS on a Tribute automatic peptide synthesizer (Protein Technologies Inc.) by using a standard 9-Fluorenylmethoxycarbonyl (Fmoc) protection peptide synthesis protocol (for details, see the ESI†). The cleavage of the peptide from the resin was achieved by using an aqueous mixture of 95% trifluoroacetic acid. The peptides were lyophilized. Three mg of lyophilized peptides were dissolved in one ml of TFA and gently stirred at 373 K for 3 hours to completely dissolve the seeds responsible for the insolubility of peptide (unseeded peptide). Upon addition of 9 ml of ultrapure water, the solution was fractionated into two equal parts and lyophilized. This procedure provided a powder aliquot for HPLC. The peptides were purified by semipreparative reversed-phase high-performance liquid chromatography on a Shimadzu automated HPLC system supplied with a semipreparative Jupiter C18 column (Phenomenex, 250x10 mm, 5 micron). Binary gradient was used and the solvents were H_2O (0.1% TFA) and CH_3CN. The purity of peptides was assessed by ESI† (Electrospray), Fourier Transformed Mass Spectroscopy (FTMS) and ^{1}H-NMR spectroscopy. (For details, refer to ESI†).

Turbidimetric assay

A time coarse measurement was carried out by UV spectroscopy on a Cary 60 UV spectrophotometer (Agilent) equipped with a Peltier temperature controller. The absorbance is expressed as TAA (Turbidity on Apparent Absorbance) as a function of time. The unseeded peptides were solubilized in TBS buffer [Tris (50 mM), NaCl (1.5 M), and $CaCl_2$ (0.5 mM) (pH 7.0)] to yield a final concentration of 1 mM, transferred by automatic pipette in one cm quartz cuvette kept under stirring at the constant temperature of 310 K. At the end of the turbidity assay, the obtained suspension was centrifuged and the supernatant was removed from the pellet. The pellet was used for AFM microscopy and FTIR spectroscopy as described in the respective paragraphs.

Atomic Force Microscopy

At the end of the turbidity assay, the suspension was centrifuged and the supernatant was removed. The pellet was washed with ultra-pure water, centrifuged and the supernatant removed. The process was repeated twice in order to remove

salts. Five microliters of the suspension were deposited on Silicon (100) wafer substrates (Aldrich, Saint Louis, Mo, USA). The silicon wafers were cleaned by using a two solvent method consisting in the immersion of the Si wafer in warm acetone bath for a period of 10 min. Then a methanol bath for a period of 5 min immediately followed with final de-ionized water rinses. The samples were air-dried and repeatedly rinsed with ultra-pure water in order to remove salts. After water evaporation, the AFM images were carried out by using the XE-120 microscope (Park Systems) in air and at room temperature. Data acquisition was carried out in intermittent contact mode at scan rates between 0.4 and 3 Hz, using rectangular Si cantilevers (NCHR, Park Systems) having the radius of curvature less than 10 nm and with the nominal resonance frequency and force constant of 330 kHz and 42 N m^{-1}, respectively, or diamond tips (Mikromasch) with typical spike curvature radius less than 7 nm, nominal resonance frequency of 325 kHz, and typical force constant 46 N m^{-1}.

Molecular dynamics simulations

All peptides were built in a fully extended conformation with phi / psi=180° and capped with Ace and NH_2 groups in N and C terminal position, respectively. All simulations were performed with NAMD 2.7 using Charmm force field, in explicit water using TIP3P model20.[43] Peptides were centred and solvated in a cubic box of approximately 46 $Å^3$. Periodic Boundary Conditions (PBC) were applied and the system was first energy minimized through 5000 steps of conjugate gradient before being submitted to an equilibration phase of 2 ns of a Langevin dynamics performed in NPT ensemble (298K; 1 atm) with Nosé-Hoover Langevin piston pressure control, and a Langevin damping coefficient of 5 ps^{-1} for all-non hydrogen atoms. Production phase of 50 ns for each peptides was performed with a damping coefficient of 1 ps^{-1}, electrostatic interactions were treated with the Particle Mesh Ewald (PME) method using a switching function applied between 11 and 13 Å. Newton's equations of motions were integrated at each 2 fs applying the Shake algorithm on all bonds involving hydrogen atoms. Coordinates were saved each 5 ps. It should be noted that the derived force field used for peptides are parametrized for globular proteins and not for unordered proteins as elastin. This finding could be responsible for possible differences between experimental and MD results. Furthermore, given the short length of peptides and in order to avoid structural biases due to electrostatic interactions occurring between the charged extremities of the polypeptide backbone, it has been preferred to cap the peptides. All simulations were performed at the "Centre de Calcul de Champagne-Ardenne ROMEO". Analyses are based on in-house scripts in R environment and on PROMOTIF tool[44] and images are produced with VMD.[45]

CD spectroscopy

CD spectra of 0.1 mg ml^{-1} solutions of unsedeed peptides were recorded at 273, 298, and 343 K on a JASCO J815 CD spectropolarimeter in water, TFE and in TFE/H_2O (80/20, v/v) mixture using a HAAKE waterbath as temperature controller and a quartz cell with a 1 mm optical path length. Samples were equilibrated for two minutes prior to measurement at each temperature. 16 scans were acquired in the range of 190–250 nm by taking points every 0.1 nm, with a 50 nm min^{-1} scan rate, an integration time of 2 s, and a 1 nm bandwidth. The CD spectra were processed using the JASCO Spectral analysis software. After background subtraction a FFT filtering algorithm was applied for smoothing, and data expressed as molar ellipticity [θ] deg cm^2 $dmol^{-1}$.

NMR spectroscopy

^{1}H NMR spectra were recorded on a Varian Unity INOVA 500 MHz spectrometer equipped with a five mm triple resonance probe and z-axial gradients. The purified peptides were dissolved in 700 microliters of TFE-d_3/H_2O (80/20), containing 0.1 mM of 3-(trimethyl-sily1)-1-propane sulfonic acid (DSS) as internal reference standard at 0 ppm. 3 mM peptide solutions were used. One-dimensional spectra were acquired in Fourier mode with quadrature detection. The residual HDO signal was suppressed by double-pulsed field-gradient spin-echo. Two-dimensional TOCSY[46] and NOESY spectra were collected in the phase-sensitive mode using the States method. Typical data were 2048 complex data points, 32 transients and 256 increments. Relaxation delays were set to 2.5 s and spinlock (MLEV-17) mixing time was 80 ms for TOCSY while 200 ms mixing time was applied to NOESY experiments. Shifted sine bell squared weighting and zero filling to 2K x 2K was applied before Fourier transformation. Amide proton temperature coefficients were usually measured from 1D ^{1}H NMR spectra recorded in 5K increments from 293 K to 318 K. Data were processed and analyzed by VnmrJ software (Agilent, Palo Alto). Sequential resonance assignments were made by the approach described by Wüthrich.[35]

FTIR spectroscopy

The samples for FTIR spectroscopy were analyzed either as lyophilized powder in the form of unseeded peptide (see peptide synthesis paragraph) or aggregated peptide as pellet (Turbidity Assay section). The lyophilized peptides and the pellets were mixed with KBr to a final concentration of approximately 1% (w:w). IR spectra were recorded on a Jasco FTIR-460 spectrometer. Each spectrum is the result of signal-averaging of 256 scans at a resolution of 2 cm^{-1} . All spectra are absorbance spectra after background subtraction. Smoothing of spectra was carried out with a step of 11 or 13 data points, using the Savitzky–Golay function.[47] Second derivatives of the spectra were obtained using a step of 13 datapoints to identify discrete absorption bands that make up the complex amide profiles. Quantitative analysis of the individual component bands of amide I was achieved by using the peak fitting module implemented in the Origins ® Software (Microcalc Inc.). In the curve fitting procedure, the Voigt peak shape has been used for all peaks. The Voigt shape is a combination of the Gaussian and Lorentzian peak shapes and accounts for the broadening present in the FTIR spectrum.

Conclusions

In this work we have compared the self–aggregation tendencies of four elastin-derived synthetic pentadecapeptides. The low molecular weight and the SPPS tool let us to obtain high yields of peptide that is mandatory for applicative use of the peptide as biomaterial. Therefore, the work contains element of novelty in comparison with previous work made on polycondensation products. Finally, from the present study, it is evident that the secondary structure is a crucial variable triggering the specific supramolecular structure adopted by the different peptides.

Acknowledgements

The authors thank the HPC–Regional Center ROMEO and the Multiscale Molecular Modeling Platform (P3M) from the University of Reims Champagne Ardenne (France) for providing CPU time and support. Thanks are due Dr. Neluta Ibris and Dr. Alessandra Scelsi for AFM images (University of Basilicata). The financial support from MIUR (PRIN 2010LSH3K) is gratefully acknowledged.

Notes and references

[a] Department of Science, University of Basilicata, Via Ateneo Lucano 10, 85100 Potenza, Italy. Fax: (+39)0971205678; Tel: (+39)0971205481; E-mail: brigida.bochicchio@unibas.it
[b] Laboratory SiRMa, UMR CNRS 7369 MEDyC, University of Reims Champagne-Ardenne, Reims, France and Multiscale Molecular Modeling Plateform, Faculty of Sciences, University of Reims Champagne-Ardenne, 51687. Reims Cedex 2, France.

† Electronic Supplementary Information (ESI†) available: [Radius of gyration of peptides, ^{1}H-NMR chemical shift assignments of polypeptides, CD of $(VGGVG)_3$ in mixture TFE/H_2O]. See DOI:10.1039/b000000x/

1 D. Mandal, A.N. Shirazib and A. N. and K. Parang, *Org. Biomol. Chem.* 2014, **12**, 3544-3561.
2 K. Schenke-Layland, H. Walles, *Biotechnol J*. 2013, **8**, 278-9.
3 A. Lakshmanan, S. Zhang, and C.A.E. Hauser, *Trends in Biotechnology* 2012, **30**, 155-164.
4 J. H. Collier and T. Segura, *Biomaterials* 2011, **32**, 4198-4204.
5 M. Reches and E. Gazit, *Phys. Biol*. 2006, **3**, S10-S19.
6 M. Reches and E. Gazit, *Science* 2003, **300**, 625-627.
7 S. Marchesan; C. D. Easton, F. Kushkaki, L. Waddington and P. G. Hartley, *Chem. Commun*. 2012, **48**, 2195-2197.
8. A.M. Tamburro, B. Bochicchio, A. Pepe 2005, *Pathol Biol*. **53**, 383-389.
9. A.M., Tamburro, V., Guantieri, D.D., Gordini, *J. Biomol. Struct. Dyn.* 1992, **10**, 441-54
10. B. Bochicchio, A. Pepe, A.M. Tamburro, *Chirality*, 2008, **20**, 985-994.
11 H. Broch, M. Moulabbi, D. Vasilescu, A.M. Tamburro, *Int J Pept Protein Res.* 1996, **47**, 394-404.
12. M. A., Castiglione Morelli, M. DeBiasi, A. DeStradis and A.M. Tamburro, *J. Biomol. Struct. Dyn.* 1993, **11**, 181-90.
13. M. Martino, A. Coviello and A.M. Tamburro, *Int. J. Biol. Macromol.* 2000, **27**, 59-64.
14 A.M. Salvi, P. Moscarelli, G. Satriano, B. Bochicchio, J.E. Castle. *Biopolymers*, 2011, **95,** 702-21
15 A.M. Salvi, P. Moscarelli, B. Bochicchio, G. Lanza, , J.E. Castle. *Biopolymers*, 2013, **99**, 292-313.
16 R., Flamia, P.A., Zhdan, M. Martino, J.E. Castle and A.M, Tamburro, *Biomacromolecules* 2004, **5**, 1511-1518
17 K.K. Kumashiro, T.L. Kurano, W.P. Niemczura, M. Martino, A.M. Tamburro, *Biopolymers*, 2003, **70**, 221-226
18 K. Ohgo, WP Niemczura, J. Ashida, M. Okonogi, T. Asakura, KK Kumashiro, *Biomacromolecules*, 2006, **7**, 3306-10.
19 P. Moscarelli, F. Boraldi, B. Bochicchio, A. Pepe, A.M. Salvi and Quaglino, *Matrix Biology* 2014, **36**, 15-27
20 J.M., Andreu and S. Timasheff, *Methods in Enzymology* 1986, **130**, 47-59.
21 B.O'Nuallain, A.K. Bhakur, A.D. Williams, A.M. Bhattacharyya, S. Chen, G. Thiagarajan and R. Wetzel, *Methods in Enzymology* 2006, **413**, 34-74.
22 J.E. Castle, A.M. Salvi,N. Ibris, N., P. Moscarelli, B. Bochicchio and A. Pepe, *Surf. Interface Anal*. **2014,** 44, 246 - 257.
23 G. Zandomeneghi, M.R. Krebs, M.G. McCammon and M. Fändrich, *Protein Sci*. 2004, **13**, 3314–3321.
24 W.K. Surewicz, H.H. Mantsch and D. Chapman, *Biochemistry* 1993, **32**, 389–394.
25 M. Martino, A. Bavoso, V. Guantieri, A. Coviello and A.M. Tamburro, *J. Mol. Struct.* 2000, **768**, 173–189.
26 S. Cai and B.R Singh, *Biochemistry* 2004, **43**, 2541–2549.
27 J. Bandekar, *Biochim. Biophys. Acta*, *Protein Struct. Mol. Enzymol*. 1992, **1120**, 123–143.
28 S. Baud, L. Duca , B. Bochicchio , B. Brassart , N. Belloy , A. Pepe , M. Dauchez , L. Martiny and L. Debelle, *BioMol Concepts* 2013; **4**, 65–76
29 B. Bochicchio, N. Floquet, A. Pepe, A.J.P. Alix and A.M. Tamburro, *Chem. Eur. J.* 2004, **10,** 3166-76.
30 F. Lelj, A.M. Tamburro, V. Villani, P. Grimaldi and V. Guantieri, *Biopolymers* 1992, **32**, 161-72.
31 A.M. Tamburro, V. Guantieri, L. Pandolfo and A. Scopa, *Biopolymers* 1990, **29**, 855-70.
32 B. Bochicchio and A.M. Tamburro, *Chirality* 2002, **14**, 782-92.
33 A.M. Tamburro, A. Pepe, B. Bochicchio, *Biochemistry* 2003, **42**, 13147-62.
34 M.A.Castiglione Morelli, A. Scopa, A.M. Tamburro and V. Guantieri, *Int. J. Biol. Macromol*. 1990, **12**, 363–368.
35 K. Wüthrich, NMR of Proteins and Nucleic Acids. Wiley: New York, 1986.
36 D.S. Wishart, B.D. Sykes and F.M. Richards, *Biochemistry* 1992, **31**, 1647-51.
37 C.J. Bowerman, W. Liyanage, A. J. Federation and B.L. Nilsson, *Biomacromolecules* 2011, **12**, 2735-2745.
38 G.G. Tartaglia and M. Vendruscolo, *Chem. Soc. Rev.* 2008, **37**, 1395–1401.
39 A.T. Petkova, W.M. Yau, R. Tycko, *Biochemistry* 2006, **45**, 498-512.
40 A.M. Fernandez-Escamilla, F. Rousseau, J. Schymkowitz and L. Serrano, *Nat. Biotechnol*. 2004, **22**, 1302-1306.

41 K. Karunakar, C.L. Hoop, K. Drombosky, K.W. Baker, R. Kodali, I. Arduini, P.C. van der Wel, W.S. Horne, R. Wetzel, *J.Mol. Biol.* 2013, **425**, 1183-1197.
42 A.V. Kajava, U. Baxa, A.C. Steven, *FASEB J* 2010, **24**, 1311-1319.
43 J.C. Phillips, R., Braun, W., Wang, J., Gumbart, E., Tajkhorshid, E., Villa, C., Chipot, R. D., Skeel, L., Kale and K. Schulten, *Journal of Computational Chemistry* 2005, **26,** 1781-1802.
44 R Core Team, R Foundation for Statistical Computing, Vienna, Austria, 2014. (http://www.R-project.org).
45 W., Humphrey, A. Dalke and K. Schulten, K. *J. Molec. Graphics* 1996,**14**, 33-38.
46 L. Braunschweiler, and R. R. Ernst, *J. Magn. Reson*. 1983, **53**, 521–528.
47 A. Savitzky and M. J. E. Golay, *Anal. Chem.* 1964, **36**, 1627–1639.1

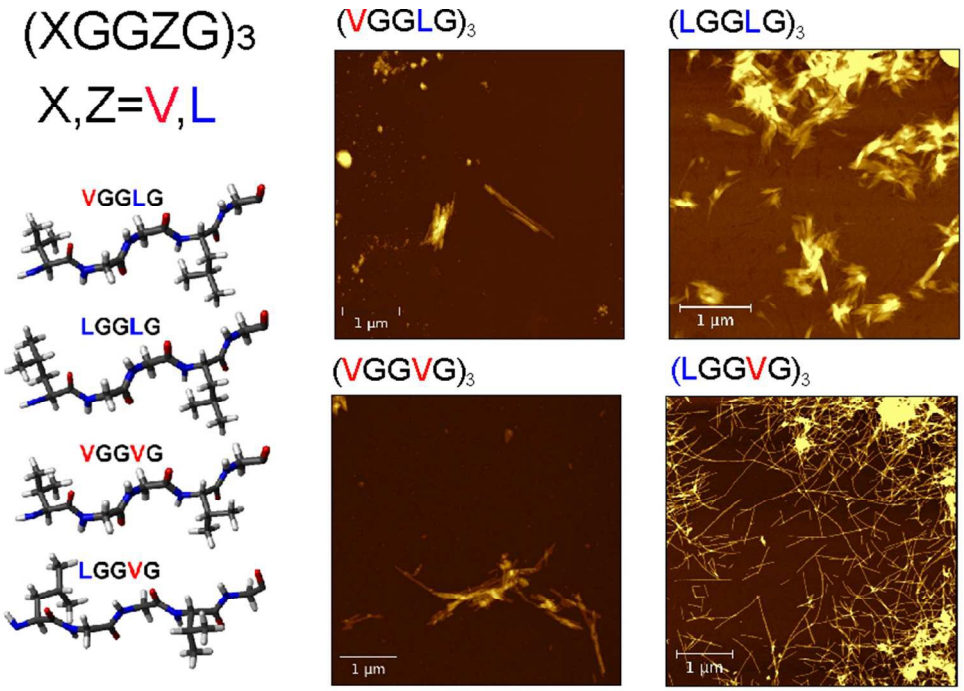

Elastin-derived peptides as bioinspired materials with predictable architectures.